

the Solid Earth, 2008, Vol. 44, # 7, pp.577–592. © Pleiades Publishing, Ltd., 2008. Original Russian Text published in *Fizika Zemli*, 2008, # 7, pp.66–84.
Gorbatikov A.V. and Tsukanov A.A. Simulation of the Rayleigh Waves in the Proximity of the Scattering Velocity Heterogeneities. Exploring the Capabilities of the Microseismic Sounding Method, *Izvestiya, Physics of the Solid Earth*, 2011, Vol. 47, # 4, pp.354–369. © Pleiades Publishing, Ltd., 2011. Original Russian Text published in *Fizika Zemli*, 2011, # 4, pp.96–112.

4. Seismogeodynamics

4.1. Seismogeodynamics and seismic hazard prediction

V. I. Ulomov, ulomov@ifz.ru. *Schmidt Institute of the Physics of the Earth RAS. B. Gruzinskaya, 10. Moscow 123995, GSP-5, Russia.*

4.1.1. Introduction

Beginning in 2010 was marked by a number of natural disasters on a global scale. One after another powerful earthquake in the Solomon Islands (January 3), Haiti (January 12), off the coast of Chile (27 February), on the border of California and Mexico (April 4), China (April 13). Apogee were two very powerful volcanic eruptions. The largest over the past half-century eruption in Chile. Giant eruptions in Iceland suspended for several days, the aviation industry in many countries.

A powerful earthquake struck Haiti on Jan. 12, 2010. Its moment magnitude of $M_w=7.1$. Almost completely destroyed the city of Port-au-Prince - the capital and main port of Haiti. Under the ruins of the city literally disappeared into densely populated neighborhoods. Killed over 270,000 people. Millions of people were left homeless.

One of the largest earthquakes in the past half century occurred off the coast of Chile on Feb. 27, 2010. It had a magnitude of $M_w=8.8$, accompanied by a tsunami and led to numerous casualties and destruction. Its epicenter was 90 kilometers from the capital of the Bio-Bio Concepcion, the second largest city in the country after Santiago. Magnitude of the strongest aftershocks reached $M_w=8.0$. The death toll from the tsunami was minimal, since most of the inhabitants managed to escape the coast in the mountains. The earthquake on Feb. 27, 2010 was the largest after the Chilean earthquake of May 22, 1960 with $M_w=9.5$, occurred at 230 km to the south.

Extremely strong earthquakes continue as at present. The author shows that this global seismogeodynamic activation is not accidental [Ulomov, 2007, 2010]. It is also reported of the prediction of strong earthquakes in the North Caucasus [Ulomov, 2006].

4.1.2. On the variation of global seismogeodynamics

The results obtained by the author are based on the study of the Earth's seismogeodynamic regime according to which the flow of seismic events is analyzed not integrally but in magnitude intervals reflecting the geodynamics of the hierarchical fault–block structure of the geological medium.

In this section of the report the sequences of large earthquakes that occurred throughout the Earth in the period from January 1996 to May 2010 were the subject of study. These earthquakes were differentiated in the magnitude intervals $M=8.5\pm 0.2$, $M=8.0\pm 0.2$, $M=7.5\pm 0.2$ and $M=7.0\pm 0.2$, completely overlapping a wide energy range, from $M=6.8$ to $M=8.7$. The last interval also included several large earthquakes of $M\geq 8.8$. (Further all of the magnitude of M correspond to M_s .)

Fig.4.1.1 shows the position of all seismic sources. Red painted sources, located at the depth of 70 km or less; blue color shows the sources deeper 70 km. These earthquake sources coincide with zones of subduction. Date of show only those earthquakes that are cited in the text. Open circles delineated foci of earthquakes in Alaska (1964) and Chile (1960). Thin red lines - the boundaries between lithospheric plates.

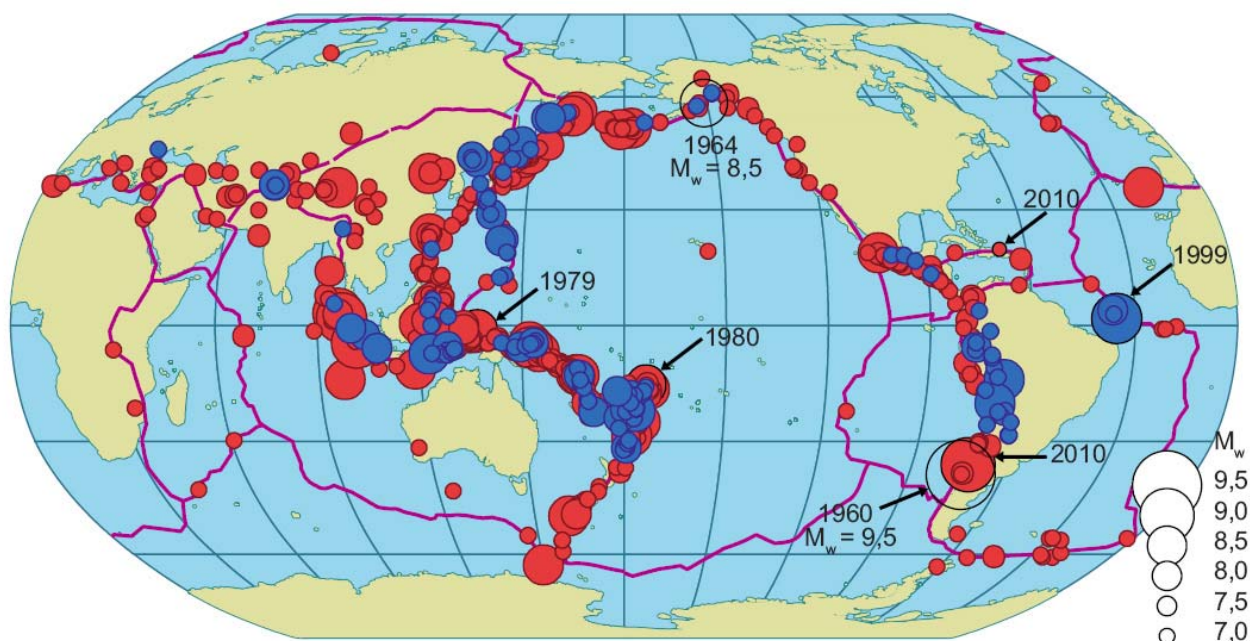


Fig.4.1.1. The epicenters of major earthquakes of the Earth for the period from January 1966 to May 2010. Scale of earthquake magnitude is shown at the bottom to the right [Ulomov, 2010].

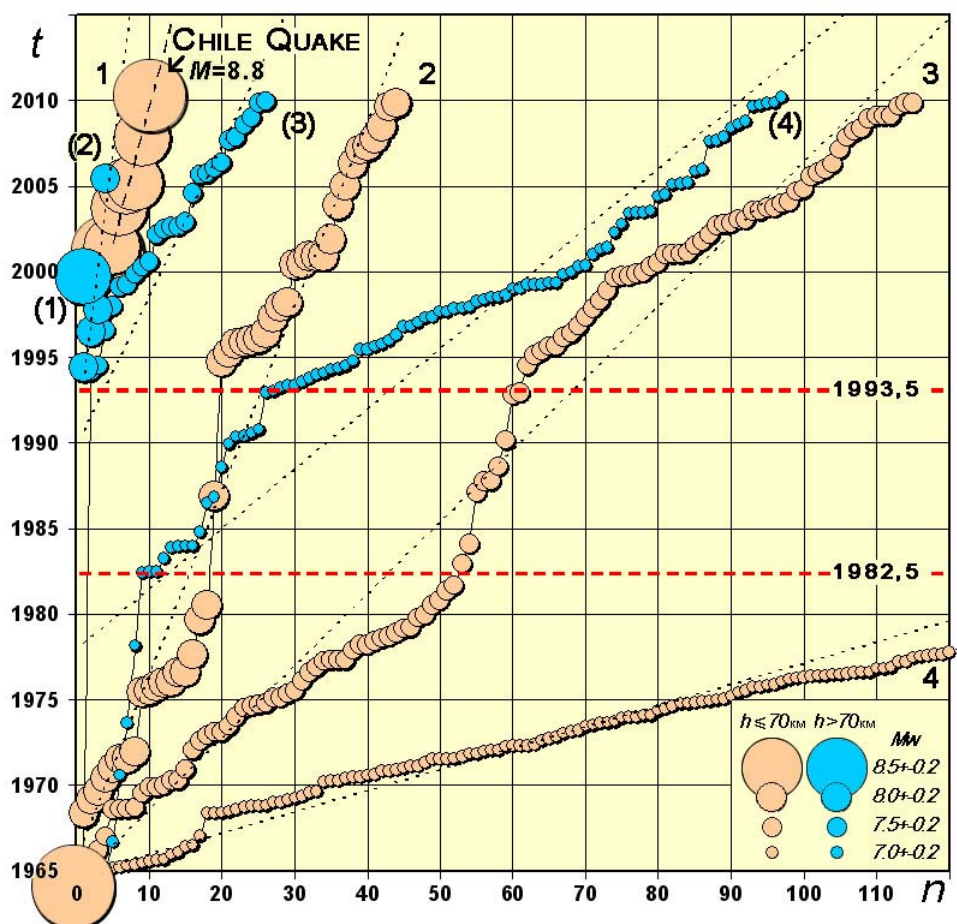


Fig.4.1.2. Cumulative plots of the accumulation of global seismic events with the magnitudes 8.5 ± 0.2 , 8.0 ± 0.2 , 7.5 ± 0.2 , and 7.0 ± 0.2 that occurred in the period from January 1966 to May 2010 [Ulomov, 2010]: 1–4 - linear approximation of the occurrence times of earthquakes with hypocenters no deeper than $h=70$ km; (1) – (4) the same for seismic events with hypocenters at depths $h>70$ km.

Cumulative plots characterizing the accumulation rate of seismic events all over the Earth in the studied magnitude intervals are presented in **Fig.4.1.2**. It should be noted that this figure, as in **Fig.4.1.1**, borrowed from the paper, which was submitted for the publication in 2007 and in this article is completed until May 2010 [Ulomov, 2007, 2010].

In **Fig.4.1.2** the cumulative number of earthquakes and the years of their occurrence are plotted on the abscissa and ordinate axes, respectively. Events with hypocenters in the depth ranges $h \leq 70$ km (shallow events) and $h > 70$ km (deep events) are shown by rose and blue color circles, respectively. The linear approximations (dotted lines) are actually everywhere characterized by the high correlation coefficient (0.9 or higher)

Because of a very large number of shallow earthquakes with $M=7.0 \pm 0.2$, only the fragment of the corresponding plot is presented in the inset in **Fig.4.1.2** (line 4).

The slopes of the approximating lines characterize the accumulation rates of seismic events of the corresponding magnitudes: the smaller the slope of a line, the higher the rate. A steepness increase reflects a decrease in the recurrence rate of earthquakes. If earthquakes occurred rhythmically, i.e., with the same frequency in each sequence, all their occurrence times, in particular, during the entire period under consideration, would lie exactly on straight lines. However, in reality, deviations from this pattern are caused by a nonlinear development of seismogeodynamic processes affecting the stress–strain state of the medium and, accordingly, seismicity manifestations.

Analysis of the configurations of the cumulative plots revealed an interesting phenomenon reflecting specific features of the temporal evolution of global seismogeodynamic processes. First of all, we mean a substantial slowdown in the recurrence of all shallow earthquakes during the approximately 11-yr time interval (from the middle of 1982 through the middle of 1993) bounded by the horizontal dashed lines in **Fig.4.1.2**. As is seen from the figure, the accumulation rates of events in the considered magnitude intervals change rather rapidly, which is expressed in abrupt bends in all plots at the ends of the anomalous interval (1982.5–1993.5). However, before and after there veiled relative seismic quiescence, the occurrence frequency of shallow earthquakes not only was substantially higher but also was characterized by virtually the same accumulation rate of seismic events.

In order to compare the occurrence frequencies of earthquakes within the magnitude ranges under consideration, the numbers of events in 11-yr time intervals before (1971.5–1982.5), during (1982.5–1993.5), and after (1993.5–2005.5) the seismic quiescence are given in the **Table 4.1.1**.

Table 4.1.1

Hypocentral depths $h \leq 70$ km				
У, годы	$M=7.0 \pm 0.2$	$M=7.5 \pm 0.2$	$M=8.0 \pm 0.2$	$M=8.5 \pm 0.2$
1993.5–2005.5	141	39	17	4
1982.5–1993.5	40	9	1	0
1971.5–1982.5	111	36	12	0
Hypocentral depths $h > 70$ km				
1993.5–2005.5	53	12	4	1
1982.5–1993.5	22	0	0	0
1971.5–1982.5	2	0	0	0

In all cases, the time is measured from the middle of the year, as in the anomalous period of seismic quiescence. It is seen that, in the interval 1982.5–1993.5, earthquakes with $M=7.0 \pm 0.2$ and 7.5 ± 0.2 occurred three to four times, and earthquakes with $M=8.0 \pm 0.2$ ten or more times, less frequently than in the preceding and subsequent 11-yr periods. The largest seismic events with $M=8.5 \pm 0.2$ and more, which were altogether absent during the first two intervals, started to occur nearly annually from 2001 through 2006. They included the catastrophic earthquakes of December 26, 2004, with $M=8.8$ and March 28, 2005, with $M=8.5$, which occurred off the Sumatra coast. The previous 1964 Alaska earthquake with $M=8.5$ was equally large, and the time interval under consideration began actually from this earthquake.

The fact that deep seismic activity began immediately after the general quiescence of the shallow seismicity is no less important (see Fig. 4.1.2). No earthquakes with magnitudes $M=7.5\pm 0.2$ and higher were observed before this period, whereas twelve earthquakes with $M=7.5\pm 0.2$, four earthquakes with $M=8.0\pm 0.2$, and one earthquake with $M=8.8$ occurred in the conclusive time interval. The last earthquake was unique in its magnitude and occurred in the Atlantic Ocean at a depth of about 90 km off the eastern coast of South America (see Fig.4.1.1). However, earthquakes with $M=7.0\pm 0.2$ occurred very seldom up to their conclusive active stage. Thus, while five such earthquakes occurred annually from the middle of 1993 and later, their recurrence rate in the period of seismic quiescence was lower by a factor of 2.5 (and before, even by a factor of 26.5).

It is noteworthy that during this same time period (1982.5-1993.5) were also found abnormal changes in global Ocean level. According to the author, these anomalies were caused by slow deformation of the oceanic lithosphere [Ulomov, 2007].

4.1.3. Reflection of the global seismicity at the regional level

No less remarkable that similar anomalies in the seismic regime at the same time interval (1982.5-1993.5 years) we found in the Caspian region [Ulomov, 2007], but for smaller magnitudes of local earthquakes (see Fig.4.1.3).

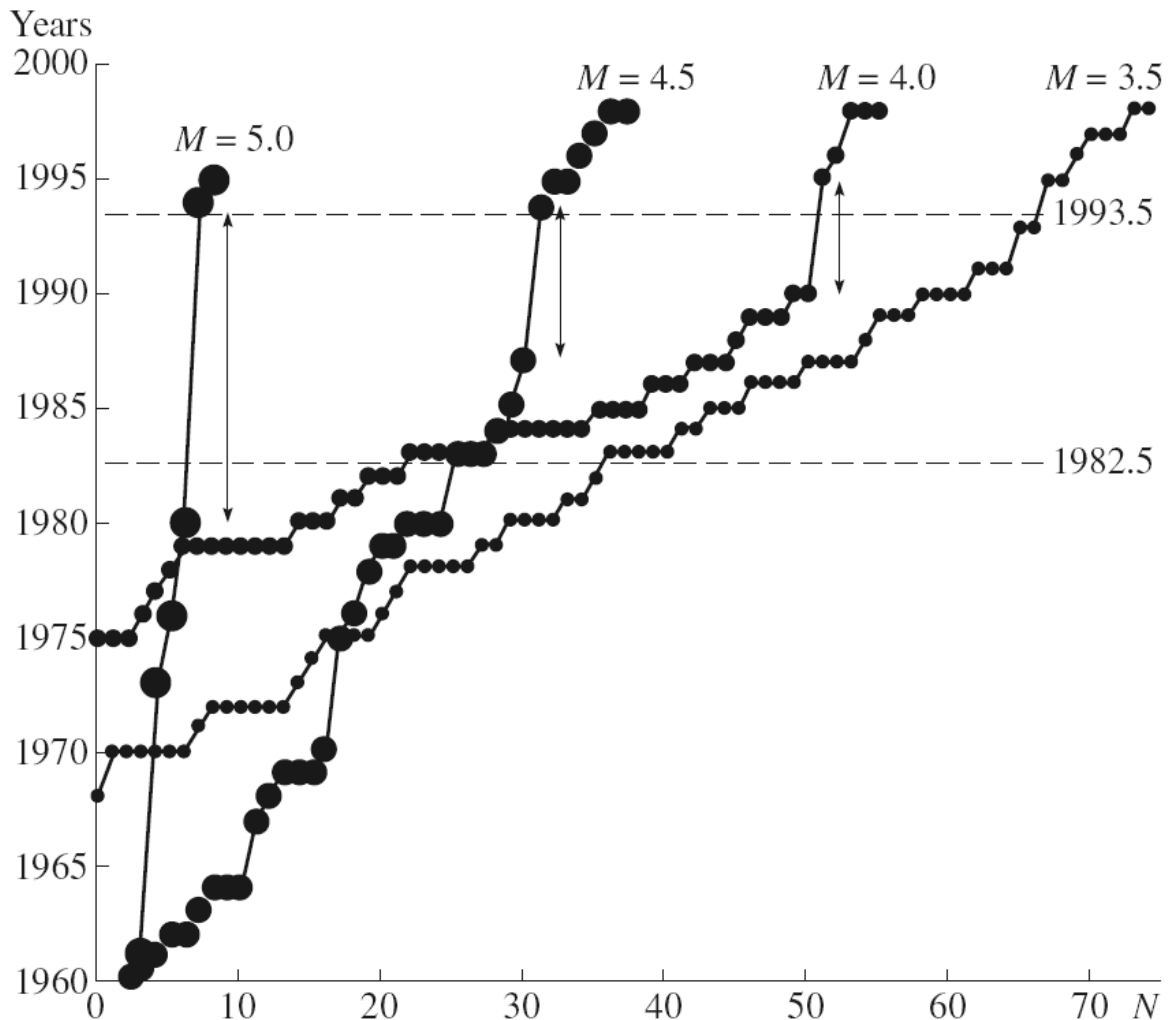


Fig.4.1.3. Sequences of seismic events of moderate and low magnitudes in the subduction zone of the Central Caspian region [Ulomov, 2007]. The time interval 1982.5–1993.5 of the global seismic quiescence is bounded by horizontal dotted lines.

A further search for the correlation between seismogeodynamic and hydrogeodynamic processes in water areas of the Caspian Sea and the Ocean should take into account the dimensions of earthquake sources and their distance from water basins. It cannot be ruled out that powerful global geodynamic processes affected in some way the Iran–Caucasus–Anatolian region, including the closed Caspian basin. One should also pay attention to a certain seismic quiescence in nearly the same time interval (1982.5–1993.5) in relation to moderate and weak earthquakes with $M=5.0\pm 0.2$, 4.5 ± 0.2 , 4.0 ± 0.2 , and 3.5 ± 0.2 in the subduction zone of the central Caspian Sea.

With decreasing magnitude, these anomalous zones become gradually less contrasting and even completely disappear in the sequence of the weakest earthquakes ($M=3.5\pm 0.2$). Incidentally, this fact emphasizes once more that it makes no sense to search for anomalies in the seismic regime of some or other region and the Earth as a whole by summing up the total number of earthquakes without their differentiation by magnitudes because an infinite set of weak seismic events will smooth the general pattern.

4.1.4. The prediction of seismic activity in the North Caucasus

Through our many years of research in the North Caucasus have been identified potential foci of strong earthquakes. The most probable location of one of them was expected in the coming years in the eastern part of the North Caucasus, on the border of Chechnya and Dagestan.

This strong earthquake with the moment magnitude $M_w = .9$ occurred on Oct. 11, 2008 in the Chechen Republic. It was accompanied by the loss of life and extensive destruction. Presented here (Fig.4.1.4) map seismogeodynamics and forecast seismic hazard in the east of the North Caucasus is taken from the publication [Ulomov, 2006]. Shown on the map of seismic sources correspond to the Specialized Earthquake Catalog of Northern Eurasia (SECNE, ed. V.I. Ulomov), composed on the basis of unified catalog of earthquakes for the period from ancient times to 2006.

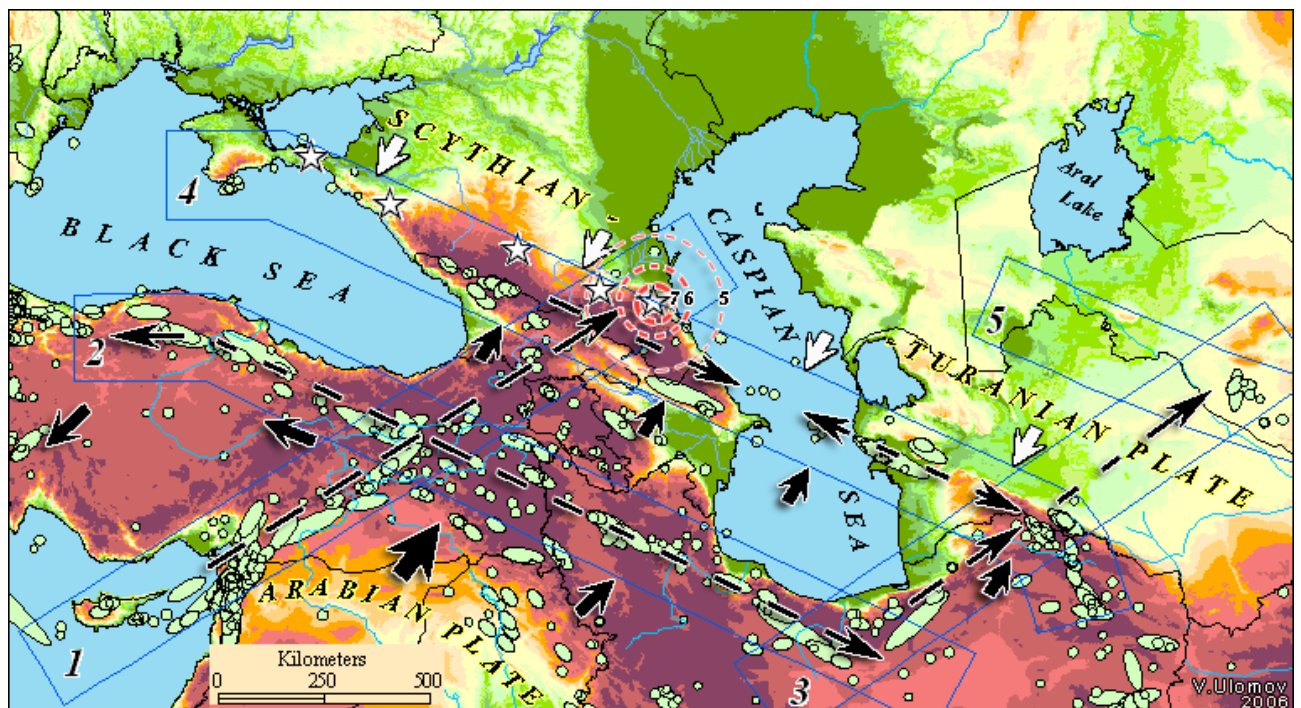


Fig. 4.1.4. The map of prediction of a strong earthquake in the eastern part of the North Caucasus, published in [Ulomov, 2007]. Potential sources of earthquakes, the stars are shown.

The Iran-Caucasus-Anatolian region, a fragment of which is shown here on the map represents a single seismogeodynamic system that makes the seismic regime throughout the territory. Studies of spatiotemporal and energy development seismogeodynamic processes along the main seismogenic structures (1. Cyprus-Caucasus, 2. Anatolia-Iran, 3. Iran-Turan, 4. Crimea-Caucasus – Kopet-Dagh) showed distinct patterns in the sequence of seismic events of different magnitudes and in the migration

of seismic activity along each of the featured structures. The direction of migration of earthquakes along the profiles indicated by the dashed arrows. Large arrows illustrate the directions of interaction between the Arabian and Eurasian tectonic plates. Conditional isoseismals in the east of the North Caucasus illustrate published in 2006-2007 [Ulomov, 2007]. anticipated effect of seismic intensity of 8-9 points.

4.1.5. Conclusion

The beginning of 2010 marked the intensification of research on the actualization of seismic normative documents in the Russian Federation - namely, building codes and zoning maps of seismic hazard. The initiators of these studies was the Ministry of Regional Development in Russia and Schmidt Institute of Physics of the Earth of Russian Academy of Sciences.

Will be harmonized research on the general, detailed and micro seismic zoning. New maps of general seismic zoning GSZ-2012 will include an assessment of seismic hazard in terms of acceleration of ground strong motion and other quantitative parameters.

The Unified Information System "Seismic Safety of Russia" in the Internet will be created.

References

Ulomov V.I. Global Changes in the Seismic Regime and Water Surface Level of the Earth // ISSN 1069-3513, Izvestiya, Physics of the Solid Earth, 2007, Vol. 43, No. 9, pp.713–725. © Pleiades Publishing, Ltd., 2007. Original Russian Text © V.I. Ulomov, 2007, published in Fizika Zemli, 2007, # 9, pp. 3–17.

Ulomov V.I. On the question of planetary seismic activity // Journal "GeoRisk", № 3, 2010. pp.4-9.

Ulomov V.I. Seismogeodynamics and seismic hazard prediction // National Report of the International Association of Seismology and Physics of the Earth's Interior International Union of Geodesy and Geophysics 2003-2006. 2007. pp.47-51.

4.2. Seismo-geodynamic applications of satellite data

V. O. Mikhailov, mikh@ifz.ru, A. N. Nazaryan, E. A. Kiseleva, E. I. Smol'yaninova, E. P. Timoshkina, Schmidt Institute of the Physics of the Earth RAS. B. Gruzinskaya, 10. Moscow 123995, GSP-5, Russia; M. Diament, N. Shapiro, IGP, Paris, France.

Introduction.

We report the analysis of co-seismic and post-seismic deformations in the region of the Altai (Chuia) earthquake of September 27, 2003. This earthquake is well studied by ground and satellite methods including images of Synthetic Aperture Radar (SAR) interferometry [Nissen *et al.*, 2007; Barbot *et al.*, 2008, Nazaryan *et al.*, 2008, Mikhailov *et al.*, 2010]. In our study, we perform joint inversion of the SAR interferometry and satellite geodesy data published in [Gol'din *et al.*, 2005]. For the purposes of a combined inversion, we developed inversion technique which allows for particular features of the geodetic and SAR interferometry data available.

Altai 27/09/2003 earthquake.

According to the refined data of the Information and Processing Center of the Geophysical Survey of the RAS and the European–Mediterranean Seismological Centre (EMSC) the coordinates the main seismic event epicenter are 49.97°N, 87.77°E. The focal depth was estimated by different seismological centers as 16–18 km and the magnitude of the main shock was 7.0–7.3. The main seismic event was followed by numerous aftershocks. Two large events of 6.2 and 6.6 in magnitude hit the region on the day of the main event and on October 01, 2003 at the northwestern extension of the main rupture [Starovoit *et al.*, 2003; NEIC data]. Analyzing the seismograms, Nissen *et al.* [2007] identified one more seismic event, which occurred presumably south-eastwards of the epicenter of the main event with the magnitude about 6.7 (Fig.4.2.1) what was confirmed by the seismotectonic observations and SAR interferometry data.